



# Detecting change in coral reef 3D structure using underwater photogrammetry: critical issues and performance metrics

P. Rossi<sup>1</sup> · C. Castagnetti<sup>1</sup> · A. Capra<sup>1</sup> · A. J. Brooks<sup>2</sup> · F. Mancini<sup>1</sup>

Received: 16 January 2019 / Accepted: 15 April 2019 / Published online: 26 May 2019  
© Società Italiana di Fotogrammetria e Topografia (SIFET) 2019

## Abstract

This paper presents a multi-temporal underwater photogrammetric survey of a reef patch located in Moorea, French Polynesia, designed to detect a coral growth of 10–15 mm/year. Structure-from-Motion photogrammetry and underwater imagery allows the three-dimensional quantification of reef structural complexity and ecologically relevant characteristics at the patch scale. A high degree of accuracy and fine resolution are required in order to guarantee the repeatability of surveys over time within the same reference system, meaning a proper geodetic network and acquisition scheme are mandatory. Measuring tools and reference points were properly designed in order to constrain the photogrammetric reconstruction. The network adjustment, performed with distance and height difference observations, provided an average accuracy of  $\pm 1.2$  mm and  $\pm 2.9$  mm in the horizontal and vertical components, respectively. The final accuracies of photogrammetric reconstructions are on the order of 1 cm and few millimeters for the 2017 and 2018 monitoring campaigns, respectively. This results in realized errors in the comparison of about  $\pm 1$  cm. Coordinate variations larger than this magnitude can be reasonably interpreted as coral growth or dissolution. The direct comparison of the two subsequent point clouds is effective in order to evaluate trends in growth and perform morphometric analyses. For highly accurate quantitative assessment of local changes, an expert operator can create and analyze specific 2D profiles that are easily produced from the point clouds.

**Keywords** Underwater photogrammetry · Coral growth · Change detection · Accuracy assessment · Deformation monitoring

## Introduction

Coral reefs have declined globally over the past several decades in response to anthropogenic threats such as warming ocean temperatures and decreasing ocean pH (Bellwood et al. 2004; Fabricus et al. 2017; Gardner et al. 2003; Hughes et al. 2017; Pennisi 2002). At local-to-regional scales, coastal development, destructive fishing practices, and pollution phenomena also have contributed to a loss of reefs (Cinner et al. 2018; Mora 2008; Suchley and Alavarez-Filip 2018).

A range of survey methodologies including satellite sensing, airborne investigations, vessel-based acoustic and light detection and ranging (LIDAR) technologies (Collin et al. 2018),

visualizations using underwater robotic vehicles (Kocak and Caimi 2005; Johnson-Roberson et al. 2010), and in situ operations based on underwater photogrammetric surveying (Burns et al. 2015; Royer et al. 2018) have been used to document declining trends in coral reef cover. These studies have focused on the description of biogenic habitats and characterizing factors at varying spatial scales and levels of image resolution. However, while remote sensing enables the investigation of large extents of reef areas, the costs to obtain the imagery can be quite high. Further, boat-based surveys can be difficult to conduct in shallower waters or in areas with high coral cover due to difficulties in accessing these areas and unfavorable acquisition geometry. Increasingly, field surveys of coral reefs carried out by robotic vehicles (Johnson-Roberson et al. 2010) or divers equipped with consumer-grade cameras are now allowing the three-dimensional (3D) quantification of ecologically relevant characteristics at the patch scales and have opened the way to obtaining detailed and accurate surveys for the monitoring of coral growth, reef structural complexity (Ferrari et al. 2017), and as predictors of reef organismal abundance, biomass, and diversity (Burns et al. 2015).

✉ P. Rossi  
paolo.rossi@unimore.it

<sup>1</sup> Department of Engineering “Enzo Ferrari”, University of Modena and Reggio Emilia, via Pietro Vivarelli 10, 41125 Modena, Italy

<sup>2</sup> Coastal Research Center, Marine Science Institute, University of California, Santa Barbara, CA 93106-6150, USA

Conventional ecological studies of coral reefs with two-dimensional (2D) planar surveys are inadequate in the delineation of most of the abovementioned characteristics due to difficulties in the quantitative assessment of parameters which are based on 3D features. On the contrary, morphometric characteristics such as rugosity and colony shape volume and surface area could be better quantified by suitably accurate 3D surveys at appropriate spatial scales (Reichert et al. 2016). Moreover, 3D metrics could provide useful information on the ability of a diversity of organisms to use corals as shelter as well as the influence of reef structure on local hydrodynamics and the amount of light received by the coral colony (Collin et al. 2018; Palma et al. 2017; Lenihan et al. 2015; Hattori and Shibuno 2015). To date, difficulties in collecting 3D data at even modest spatial scales of 1 to 10s of meters has limited the usefulness of these studies. Also, relatively few studies have been carried out to quantify the precision and accuracy of the metrics derived from 3D models of coral reef habitat structural complexity (for examples, see Bryson et al. 2017; Ferrari et al. 2016).

In recent years, thanks to the use of Structure-from-Motion (SfM) photogrammetry, images acquired by unmanned underwater vehicle and divers can be used for the reconstruction of geomorphic features, archeological sites, and benthic communities at cm-to-mm spatial resolution, depending on the camera settings used and the distance to the imaged object (Capra et al. 2017, 2015; Drap et al. 2013; Sarakinou et al. 2016). The general SfM workflow and the achievable accuracy have been documented in many papers based on aerial and ground-based surveys (see Agüera-Vega et al. 2016; Eltner et al. 2016; Fonstad et al. 2013; Harwin et al. 2015; Mancini et al. 2013; Nex and Remondino 2014; Rupnik et al. 2014; Toschi et al. 2013 among others). These studies reported that absolute positional accuracies of the 3D models were achievable at the cm level when a reliable reference frame was established using ground control points (GCPs) that had been surveyed using methods accurate enough to generate standard deviations ranging from several millimeters to 1 cm.

Little has been published about the metric accuracy of 3D models obtained by the processing of datasets containing underwater images based on the SfM approach. As such, it represents a fundamental topic for studies devoted to monitoring tasks by multi-temporal photogrammetric surveys of coral reef complexity. Figueira et al. (2015) evaluated the precision (by repeated surveys) and accuracy (using a laser reference model as a benchmark) of 3D models representing marine benthic habitat by underwater photogrammetry at the coral colony and patch reef spatial scales. Using off-the-shelf equipment in the replication of surveys in a controlled environment, they found average differences in colony morphology of 1–6 and 25 mm for patch reef areas. Information about the accuracy achieved by the underwater photogrammetric surveys is essential whenever these data are planned for monitoring purposes and plays

a crucial role in future studies aimed at determining the rate of growth and changes detection from multi-temporal underwater photogrammetric surveys.

In the monitoring of growth or loss in coral 3D structure and from the surrounding environments at the patch scale, 3D models and shapes obtained from multi-temporal photogrammetric datasets must be keyed to a common reference frame in order to allow for successive comparisons. Such a comparison procedure must be accurate enough to precisely detect typical rates of changes occurring in the structural properties of corals on the order of 1 cm/year (Bessat and Buigues 2001; Skarlatos et al. 2017; Neyer et al. 2018). The choice of an accurate reference frame and the implementation of the operational condition is still an open problem in the upcoming application of underwater photogrammetry to coral health.

This study presents photogrammetric, multi-temporal surveys of a patch reef located in Moorea, French Polynesia, with the specific aim of providing a workflow for the 3D monitoring and mapping of coral reefs at the level of accuracy required to detect annual changes in the 3D structure of the reef. Because of the cm-level accuracy needed in such investigations, an accurate geodetic network must be established to guarantee a common unambiguous reference frame for further comparison of the photogrammetric models reconstructed from underwater photographic surveying over time (Guo et al. 2016). In this case, the reference frame was established by installing and surveying a high-quality underwater control network, composed of benchmarks in fixed positions. The local network adjustment produced GCP coordinates at sub-centimeter level of accuracy that were used as reference markers in the external orientation of photogrammetric models. The investigation at a patch scale,  $\sim 100 \text{ m}^2$ , was performed within the context of the Moorea Island Digital Ecosystem Avatar (IDEA).

## The Moorea IDEA project

The Moorea IDEA project was initiated in 2013 by a group of international researchers to create a digital Avatar of the island of Moorea, French Polynesia. The project involves an interdisciplinary group of experts in order to develop a system of complex relationships where ecological data and social information are assembled into a comprehensive time-evolving model of the island (<https://mooreaidea.ethz.ch/project>). Understanding and modeling complex socio-ecological systems provides a predictive, personalized, participatory approach to policy making aimed at achieving local sustainability. Moorea is strategically located in the middle of the South Pacific Ocean and offers several of the most complex ecosystems on Earth that can be studied to reveal the effects of natural and anthropogenic stressors on ecosystem processes. The precise 3D measurements of changes in the amounts and 3D structure of

living coral over time is an essential component of future investigation of the impacts of climate change (i.e., ocean warming, increases in cyclones, ocean acidification). Several tests, surveys, equipment designs, and upgrades have been carried out since the first attempts at using underwater photogrammetry in Moorea were initiated in 2015 in order to obtain 3D models with sufficient accuracy and precision to allow the monitoring of ecologically relevant reef characteristics. In this paper, we present the results of our 2017 and 2018 monitoring campaigns.

## Site description

Moorea (17° 30' S, 149° 50' W) is a high volcanic island with an offshore barrier reef and narrow (~0.8–1.5 km wide) lagoons (mean depth ~5–7 m) that surround its ~60 km perimeter. Most recently, the island's coral reefs have experienced a series of natural disturbances beginning in 2007 with a severe outbreak of crown-of-thorns sea stars (COTS). At the conclusion of the COTS infestation in 2010, the cover of live coral had declined from an island-wide average of ~40 to <5%. In February of 2010, large waves associated with a category 4 cyclone (Cyclone Oli) that passed to the southwest of Moorea removed large amounts of dead coral, primarily on the north shore of the island, effectively eliminating much of the small-scale 3D structural complexity associated with the reef (Adam et al. 2014).

The Moorea Coral Reef Long Term Ecological Research project (<https://mcr.lternet.edu>) has censused the coral reef communities of Moorea since 2005, documenting the rapid recovery of coral on the fore reefs and within the lagoons of the island since 2010 (Holbrook et al. 2016). Much of the observed coral recovery on the fore reef was driven by high levels of recruitment to the reef by coral larvae (Holbrook et al. 2018; Edmunds 2017) and rapid initial rates of increase in coral linear extension of between 1 and 3 mm mo<sup>-1</sup> (Trapon et al. 2013) and coral planar area of up to 3–5 cm<sup>2</sup> per year for corals in the genera *Pocillopora*, *Acropora*, and *Porites* (Kayal et al. 2018) have been observed. While standard diver surveys and photo-quadrats are enough to quantify patterns of coral percent cover and the degree of coral community reassembly, they are not capable of quantifying the return of reef 3D structure.

Our study area is located on the fore reef at a depth of approximately 10 m. The site is comprised of 20 5 m × 5 m experimental plots that have been monitored for live coral cover annually since 2009 was selected due to its high diversity of coral. The specific test plot investigated in this paper (Plot 17) is a part of this larger area of interest (hundreds of meters). Plot 17 is one of five sample plots that have been used for testing the performance of underwater photogrammetry for use in ongoing monitoring surveys (Fig. 1).

## Methods

Underwater photogrammetry performed by experienced divers provides a reliable technique to generate a highly accurate 3D reconstruction of a coral reef. It is a noninvasive investigative technique able to provide sufficient resolution for change detection in reef architecture resulting from coral growth and mortality. However, in order to guarantee the repeatability of photogrammetric measurements over time within the same reference framework, it is mandatory that a proper geodetic network be installed.

## Geodetic reference network

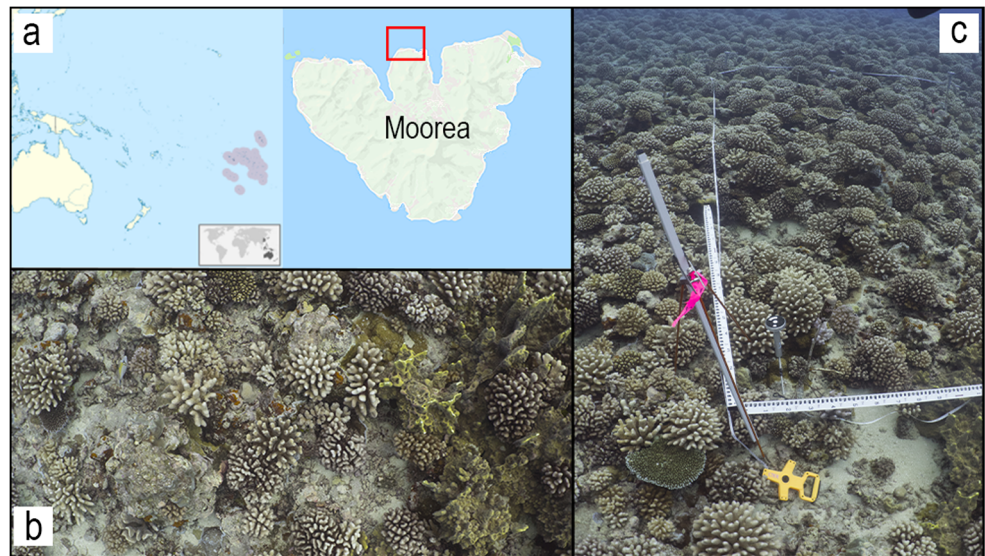
### Design and installation

The geodetic reference network is defined by means of several well identifiable points, i.e., ground control points (GCPs), with known coordinates that can be used as constraints in the photogrammetric processing and provide metric content to the generated 3D models resulting in a reduced degree of mis-orientation of images. The GCPs should (1) cover the investigated area (both in horizontal and vertical planes) as homogeneously as possible, (2) be visible in a high number of images, and (3) allow topographic measurements of the network. GCPs require an installation that is temporally constant in order to enable divers to relocate the marker in precisely the same position during future monitoring campaigns. In our study, multiple GCPs were installed by drilling into the reef matrix to a vertical depth of approximately 40 mm and permanently cementing a threaded, expansion anchor into each hole. GCPs were then deployed on the tops of 9.5 mm threaded rods screwed into the expansion anchors. GCPs were removed after each survey, but the expansion anchors were left in place for use in subsequent surveys. This design reduces the chances of loss of reference points due to a range of natural events, does not visually impact the environment and does not result in a disturbance to live coral and provides a permanent network of GCPs to enable the comparison of 3D models constructed at different time points. Our geodetic network was installed on the fore reef in 2016 and consists of five GCPs homogeneously spaced over our fore reef test plot encompassing a total reef area of 25 m<sup>2</sup> (Fig. 3).

### Equipment design and data collection

Change detection of coral reef biocenosis is a demanding application in terms of the required accuracy of the estimates of the GCP coordinates. The most common geodetic instruments used such as GNSS (Global Navigation Satellite Systems) receivers, total stations, and laser scanning cannot be used easily for surveying photogrammetric GCPs underwater. In order to obtain accurate and precise measurements of

**Fig. 1** Test site. **a** Map of the western south Pacific Ocean. The location of French Polynesia is highlighted in purple. The red square on the map of Moorea shows the approximate location of investigated area. **b** An image of the investigated coral reef. **c** Graduated surveyor rods used for the validation of the generated 3D models



distances and height differences between GCPs, we have developed several specialized pieces of equipment to deliver a practical, easy to implement, and cost-affordable solution for measuring GCPs in the underwater environment that allows the unambiguous identification of our GCPs during the image processing step. These devices include:

- A series of 9.5-mm-diameter, 30-cm-long stainless steel rods that can be screwed into expansion anchors cemented into the reef matrix. This method allows GCPs to be installed quickly on the reef for data collection, and then removed at the conclusion of the survey in order to avoid damage to or the loss of the GCPs during periods of high wave intensities on the fore reef (Fig. 2a, bottom).
- Headers devoted to the identification of the GCPs within the acquired imagery (photogrammetric target). These headers are 80 mm in diameter and 40 mm in height with a pre-printed, computer-generated black and white coded number glued to the top surface of the header (Fig. 2a, top). These headers fit into specialized adaptors (see below)
- Headers devoted to distance measurements (measuring ring) (Fig. 2b). These headers are designed with a bottom pin that fits into the specialized adaptors allowing azimuth rotations while preventing any vertical slip. This header type has a ring on the top of the header with a lateral small opening that can be used as a reference for distance observations. Distance observations are performed by means of a measuring tape with millimeter gradation.
- A number of aluminum adaptors with a diameter of 30 mm and a length of 160 mm that can be screwed onto each threaded rod and can accommodate the installation of one of two interchangeable headers devoted to the measurements of the geodetic network or to the identification

of individual GCPs within the acquired imagery (Fig. 2c). These adaptors together with threaded rods also allow the GCPs to be raised above the height of the surrounding corals making it possible to observe and measure any GCP from any other point within the network.

The two headers are designed so that the GCP target and the center of the ring used in distance measurements have the same elevation when installed on the top of the aluminum poles (Fig. 2f).

- A commercially available, underwater green laser pointer (Fig. 2d) used in conjunction with a millimeter-scale graduated leveling rod to carrying out leveling observations within the geodetic network. The laser pointer is mounted onto a standard surveyor's tripod equipped with a bubble level and then positioned between two GCPs. Aiming the laser at each GCP in succession allows divers to precisely determine the difference in elevation between the two GCPs.
- A special mounting system for the laser pointer (Fig. 2d). This mount allows the laser to be rotated and locked into one of two positions. Tests performed prior to our surveys identified a deviation in the laser pointers optical axis from the main axis of the laser housing. As a result, the location of the laser on the graduated leveling rod differs depending on the rotational orientation of the laser. To correct for this effect, two elevational measurements are taken underwater with the laser locked into successive positions oriented  $180^\circ$  relative to one another. The designed mounting system also allows for the flat, horizontal rotation of the laser through  $360^\circ$  without modifying the elevational position of the laser pointer.



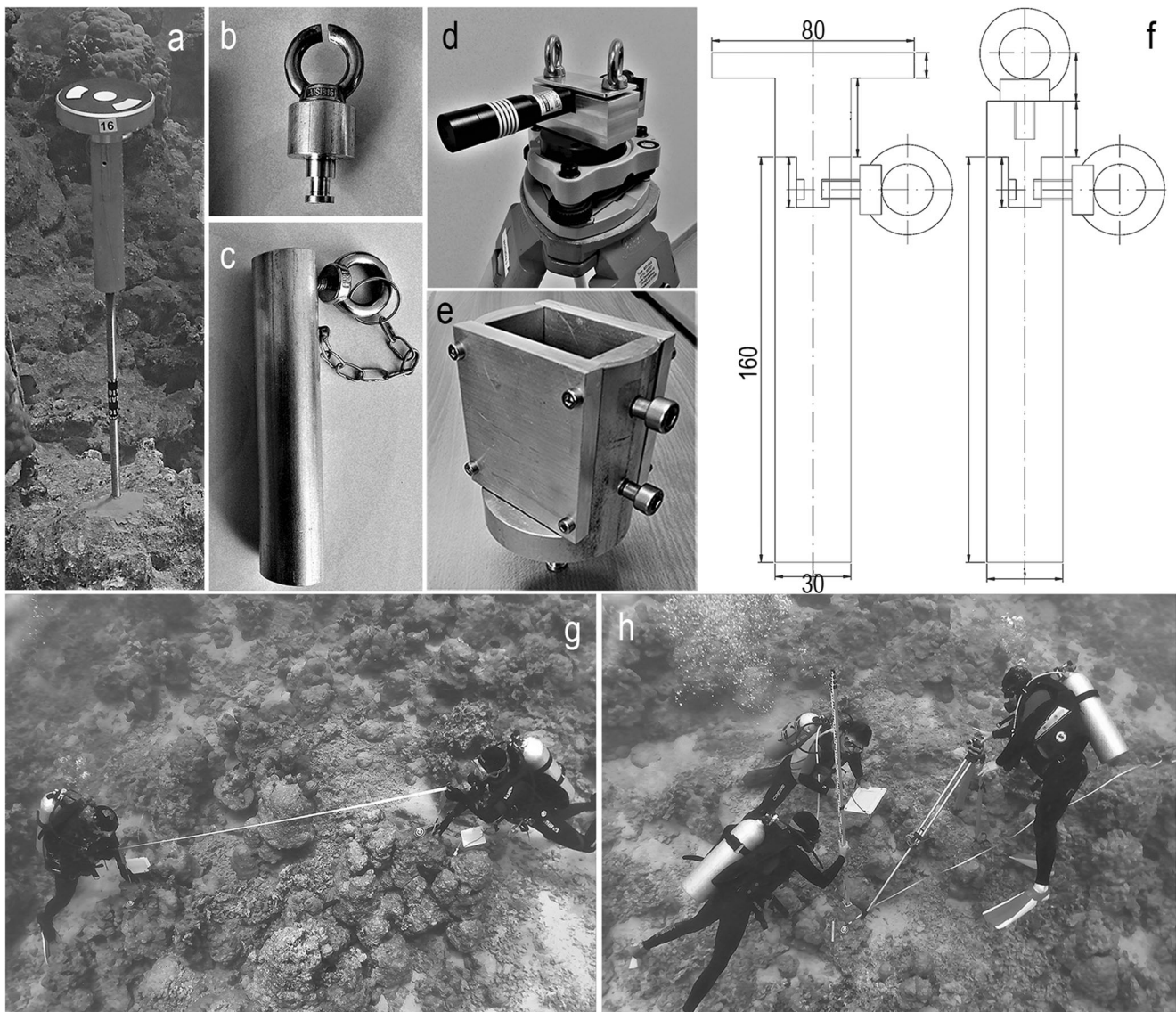


**Fig. 2** Geodetic reference network: equipment and data collection. **a** On-site installation of GCP with threaded bar, pole, and mounted photogrammetric target. **b** Measuring ring header for distance measurements. **c** Aluminum pole. **d** Laser pointer with special mounting system installed over the tripod. **e** Adapter for the leveling rod. **f** Technical drawings of the

mentioned devices (photogrammetric target header on the left, measuring ring header on the right, dimensions in mm). **g** Collection of distance measurements in operative conditions. **h** Collection of leveling observations in operative conditions

- An adapter that could be connected to the permanent anchor of each GCP. This adapter was developed for the precise positioning of the leveling rod above each GCP anchor, allowing a repeatable positioning and facilitating the ability of a diver to keep the leveling rod vertical during leveling measurements (Fig. 2e).

All devices were manufactured from aluminum in order to avoid corrosion resulting from prolonged immersion in seawater. Importantly, all adapters were manufactured to a standardized height guaranteeing that the final elevation of the assembled GCPs remained constant irrespective of the specialized header type installed. The material production cost of each unit

was about 50 euros not including design and labor costs involved in metal machining by a skilled technician. Installation of the ten stainless steel, expansion anchors for the GCPs required two divers on SCUBA approximately 1 to 1.5 h.

Several operative strategies were developed to optimize data collection and improve the final accuracy of 3D models. When measuring distances between GCPs, divers extended the measuring tape between the measuring ring adapters installed on two of the GCPs (Fig. 2g) taking care to keep the metal measuring tape taught while not bending the stainless-steel rods supporting the GCPs. All distances were measured twice, with divers alternating positions between the two GCPs. Distance measurements were made between all

sets of GCPs in order to provide a redundant set of distance observations. Leveling measurements were made by positioning the surveyor's tripod supporting the laser pointer at a point approximately equidistant to the two GCPs being measured (Fig. 2h). In this way, the residual small misalignments of the measuring device resulting from errors in vertically leveling the tripod will result in the same amount of measurement error in reading the position of the laser on the leveling rod when alternatively placed on the two expansion anchors marking each GCP. Leveling measurements required three divers; two divers to accurately position the leveling rod and read the position indicated by the laser and a third diver to position the surveyor's tripod and operate the laser. We first made measurements of our installed geodetic network on August 2017. We repeated these measurements again in August of 2018 in an attempt to improve measurement accuracy. The present paper reports GCP coordinate results we obtained in 2018 while implementing the above-described optimized protocols.

### Network adjustment

As described in the “[Geodetic reference network](#)” section, the geodetic network establishes the local reference frame which needs to be conventionally fixed by defining one GCP to act as the origin and then taking a bearing from this origin point to a second GCP (minimal constraint network). The local reference frame adopted at our fore reef test site was fixed using GCP #6 as a benchmark origin with the  $x$ -axis pointing towards GCP #9. In order to avoid negative values in the  $z$ -direction, the origin elevation was set a priori to 5.00 m (Table 1). Raw observations were first preprocessed to detect outliers and to compute the input for the network adjustment process. For each distance segment, we computed the average distance between the raw observation pairs. We then computed the elevation differences between sets of GCPs by averaging the two raw leveling readings as obtained by rotating the laser pointer. Closure errors in the network were verified by combining elevation differences in order to ideally perform our analyses on closed leveling rings. Preprocessing of the raw observations provided estimated values for the a priori standard deviations of measurement observations of 1 mm for distance observations and 5 mm for elevation differences.

The network geometry and the number of observations were sufficiently redundant to allow a high-quality computation. The whole dataset used as input for the network computation was characterized by 18 observations obtained from the sum of the average distances and differences in elevations. The geodetic network was composed of 5 benchmarks and 12 unknowns consisting of the coordinates of each GCPs except for the origin which is conventionally fixed (minimum constraint strategy). Therefore, the number of redundant observations was six. We computed a least square adjustment

using STAR\*NETPRO v. 6.0.36 Commercial Suite (Starplus Software Inc., Oakland, CA).

### Underwater photogrammetric campaigns

The photogrammetric surveys were performed annually by experienced SCUBA divers operating in depths of 12–14 m in areas of the reef characterized by coral colonies of small to medium size (~5–30 cm in diameter). Divers also installed the GCPs containing photogrammetric targets prior to image collection and periodically checked the integrity of the geodetic network.

### Image collection

Several models of cameras either singly or in multiple camera combinations were used to acquire imagery in order to test camera performance in the underwater environment and identify optimized camera settings. A Lumix DMC-GH4 and a Nauticam underwater housing equipped with a dome port to reduce the distortion effects generated by the aquatic medium (Menna et al. 2016) was used as the standard reference camera. This camera has been used by us to acquire photogrammetric imagery of reefs in Moorea since 2015 (see Fig. 1b for an example of acquired images). The reference camera was used with a nominal focal length as fixed in air of 20 mm in 2017 and 22 mm in 2018; an effective lower focal length is expected when the camera is used underwater due to the magnification effect equal to  $1/4$  produced by the water medium (Capra 1993). Short focal lengths should be avoided in order to reduce metric distortions in the acquired images and a proper underwater case and dome port should be used to reduce distortion effects due to the aqueous medium. We used an exposure time of  $1/90$  s during our 2017 survey and  $1/125$  s in our 2018 survey in order to optimize image capture and reduce motion blur. We used the camera's autofocus procedure to focus the camera and variations in the acquisition distance of the images were so slight that the autofocus setting did not produce significant changes in the focal length. Images were collected with a frame acquisition rate of  $1 \text{ s}^{-1}$  2 m above the reef surface during the 2018 campaign and 5 m above the reef during the 2017 campaign. These parameters were determined by considering the average diver swimming speed required in order to obtain an adequate ground resolution. The photographic survey was designed to guarantee the desired degree of image overlap,  $> 90\%$ , required for SfM processing (Harwin et al. 2015). Divers swam paths orthogonal with respect to the main photographic survey lines to improve photographic coverage of the imaged plot. Finally, to strengthen the image surveying geometry, both nadir and off-nadir inclinations of the main camera axis were used. The need for a high degree of accuracy in the final 3D model requires a robust acquisition geometry that was achieved by having the

divers follow a grid superimposed over the test site. This method ensured that divers acquired photographs in both longitudinal and orthogonal directions and that the images are acquired with a slightly off-nadir asset of the camera (ranging from 0° to 30°). The fore reef test area was surveyed using several different viewing angles that allowed us to improve the intersection of optic rays, detect vertical sides of corals concretions and avoid occlusions in valleys between colonies (Rossi et al. 2017). Image collection was performed under conditions of natural lighting and low current speeds to avoid shadows, suspended materials and obtain the highest quality images possible.

### Image processing and 3D model comparisons

Photogrammetric processing was performed using the SfM algorithms contained in the software package Agisoft PhotoScan v.1.3.4 to generate a 3D model reconstruction from the acquired images. When performing successive surveys, repeatability is critical to enable the comparison of the resulting 3D models. In terms of repeatability, we also recommend using the same software package and settings. Our processing workflow consisted of first removing all poor quality images (i.e., out of focus, motion blurred) from the processed dataset. Then a preliminary image orientation was performed through the automatic identification of tie points within a bundle adjustment. Tie points with a high degree of reprojection error (mainly those outside the investigated area or detected in only two images) were removed and the GCPs coded targets automatically identified in the images. The orientation of images was further refined and constrained by introducing GCP coordinates, along with their related accuracies obtained from the geodetic network adjustment (see Table 1). The refinement orientation was performed through a non-linear, least squares minimization during the bundle adjustment. The external constraints given by introducing GCP coordinates allowed us to obtain the real positions and orientations of the cameras, calculate the internal camera parameters, and generate a georeferenced 3D model. The use of a self-calibration procedure, estimating internal camera parameters based on the actual collected imagery considering real operative conditions, further served to guarantee accurate results (as demonstrated by Snavely et al. 2006). A dense point cloud was generated using a dense image matching algorithm to match pixels located on different images, thereby allowing the reconstruction of a depth map and the creation of a high-density point cloud. We use the terms “point cloud” and “3D model” synonymously to refer to the 3D reconstruction of the test plot. Only the original 3D point cloud was used in subsequent analyses as any surface modeling may introduce interpolation and smoothing effects on the reconstruction. The validation of the generated point clouds and the estimation of their final accuracies was performed by using points/objects whose coordinates/dimensions were not previously employed in the

photogrammetric processing (Toschi et al. 2013). In the present case, graduated bars with known lengths were positioned in the surveyed test area (only in 2018 dataset) prior to image collection so that they were included within our collected images and available for validation (Fig. 1c). The differences between real values and 3D reconstruction estimations of distances identified on graduated bars were used to determine the accuracy of the computed 3D point clouds. 3D models obtained from images collected in 2017 and 2018 then were compared in order to detect any significant changes in reef geometry over time. The multi-temporal comparison was performed through the calculation of cloud-to-cloud distances using the Multiscale Model to Model Cloud Comparison (M3C2) algorithm as implemented in the open source software CloudCompare v. 2.9 (Lague et al. 2013). This algorithm considers both the 3D model complexity and the point cloud noise to provide the correct calculation of distance vectors. The definition of a normal direction to the reference 3D model, along with the calculated distances between the two point clouds, is crucial as the coral reef in the tested area exhibits a great degree of 3D complexity. In order to calculate the direction for distance measurements M3C2 allows the user to define a search diameter on the reference model that creates a surface for which the normal is calculated. In this case study, the diameter varies between 0.002 m and 0.02 m according to geometrical features of the reef. The 3D distances between models were computed by defining the 3D model obtained in 2017 as the reference model and then comparing the 3D model obtained in 2018 to this reference model.

## Results

### Ground control points adjusted solutions

The final GCP coordinates and the achieved accuracies (at 68% level of confidence) are reported in Table 1. The geodetic network adjustment provided encouraging results with an average accuracy of  $\pm 1.2$  mm in the horizontal component and  $\pm 2.9$  mm in the vertical component. Figure 3 shows the adjusted results in terms of the input observations and the error ellipses for each of the GCPs (at a 95% level of confidence, exaggeration factor of 100). The ellipses are well balanced, with increasing values when moving away from the origin, as expected due to error propagation.

### 3D models

Results of the photogrammetric processing are shown in Table 2 for both the 2017 and 2018 field missions. Image orientation was performed in the processing of the imagery from both surveys by introducing the same adjusted coordinates for the GCPs (see values in Table 1). The two datasets



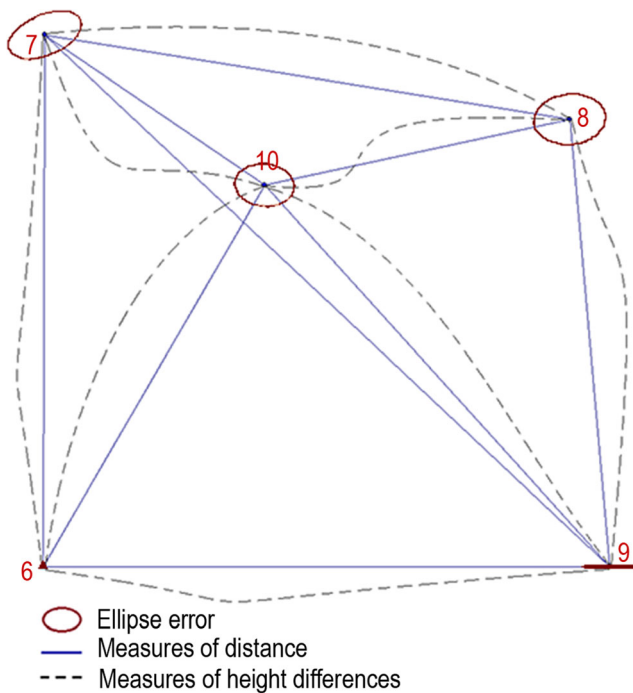


**Fig. 3** Geodetic network adjustment results. Geometry of the geodetic network with the error ellipses (95% level of confidence, exaggeration factor of 100), the observed distances (blue lines) and the leveling trajectories (dashed black lines)

differ in terms of the number of images collected and the image acquisition height above the reef. This resulted in slightly different degrees of image resolution. As shown in Table 2 (line o), both acquisitions were enough to ensure a high degree of image redundancy ( $> 9$ ), but the survey acquisition geometry was further improved in 2018 by increasing the number of times the divers passed over the reef test area. In order to reduce the differences in resolution of the generated products, a dense point cloud with high-quality settings was computed for the 2017 dataset, while medium-quality settings were used for the 2018 dataset. This strategy downscales processed images (high means a downscale factor of 4 with respect to original images size; medium indicates a factor of 16) and results in a similar number of points in the two point clouds at the expense of longer processing times (one more day is required for computing the 2017 dataset with respect to the computational burden required by 2018 dataset—Table 2, line g).

**Table 1** Geodetic network adjustment results. Resulting coordinates and accuracies (68% level of confidence)

ID	$E$ [m]	$N$ [m]	$H$ [m]	$\sigma E$ [mm]	$\sigma N$ [mm]	$\sigma H$ [mm]
6	0.000	0.000	5.000	0.0	0.0	0.0
7	0.018	5.37	4.566	1.5	1.0	3.6
8	5.323	4.519	4.316	1.5	1.0	4.1
9	5.724	0.000	4.661	1.0	0.0	3.6
10	2.238	3.854	4.811	1.2	0.9	3.4

Generated point clouds were delivered within the same reference system as defined by the geodetic network based on the adjusted GCP coordinates. The photogrammetric model not only adapts its geometry to the imposed constraints but also computes the discrepancies between imposed and estimated coordinates of the GCPs. Both datasets show average discrepancies of a few millimeters along the three directional axes, and these discrepancies are similar to the accuracies of the input GCP coordinates. The mean 3D discrepancy of the GCPs were 3.6 mm in 2017 model and only 0.4 mm in 2018 model (Table 2, line h). For both time periods, the discrepancy of each GCP was spatially displayed on a map where the error ellipse sizes represent the horizontal values of discrepancy and the error ellipse colors represent the discrepancy in elevation (Table 2, line o). The accuracy of the generated 3D models was evaluated by comparing the known lengths of graduated bars to the measured length of the graduated bars as detected within the models themselves: several lengths were identified and verified along the three main axes. The measured differences were normalized to the reference distance of 1 m and then averaged in order to obtain a representative value for the realized final accuracy. The most accurate reconstruction ( $< 1$  mm) is obtained around point 6 (origin of the reference system), while the least accurate (1.1 mm) was detected at the opposite position (areas around point 8) (Table 2, lines l-m-n).

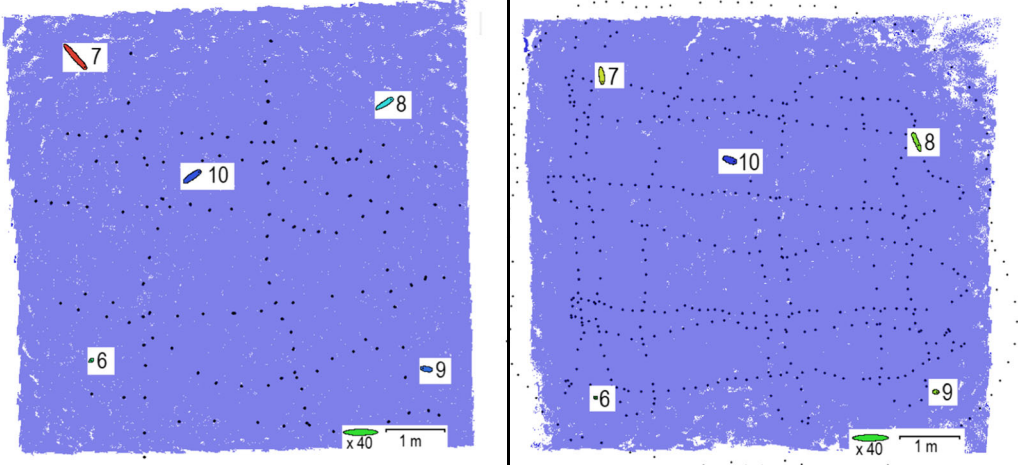
### Multi-temporal analysis

A multi-temporal analysis was performed involving the evaluation of coral growth over 1 year by calculating the oriented distances between the two 3D models using the M3C2 algorithm. The results of this comparison obtained by projecting the calculated distances on the 2017 model (previously subsampled at 0.005 m in order to speed up the computation and results analysis) are shown in Fig. 4. We obtained values ranging from  $-60$  and  $60$  mm. These values are within the range of coral growth rates observed in studies of in situ coral growth conducted on Moorea (Fig. 4a) (Traçon et al. 2013). Absolute values for coral growth at the higher end of these estimates are mainly due to errors in our distance calculation, the presence of unrelated objects, or to the loss of whole coral colonies (Fig. 4b, c).

The statistical comparison of the distribution of differences between the two 3D models shows a peak centered at approximately 5 mm and a median value of 12 mm (see right Fig. 4a). In order to investigate these results in more depth, we generated new maps showing only differences in model point clouds corresponding to values exceeding 15th and 85th percentiles. This equals positive distances values ranging from  $+35$  and  $+60$  mm (Fig. 4b), and negative distances lower than  $-6$  mm (Fig. 4c). Particularly large positive distances are well



**Table 2** Main SfM processing results: acquisition settings, number of reconstructed points, time for processing, discrepancies on GCPs, and accuracy check on graduated bars

FORE REEF, PLOT 17									
		August 2017				August 2018			
a	N° of images	148				552			
b	Diving distance	4.5 m				2.1 m			
c	Ground resolution	1.3 mm/pix				0.5 mm/pix			
d	Reprojection error	1 pix				1.1 pix			
e	Point cloud	35660000 points(*)				33550000 points(**)			
f	Orientation	1 hour				11 hours 30 minutes			
g	Dense Cloud	1 day 20 hours(*)				20 hours(**)			
h	Discrepancies on GCPs (average values)	X [mm]	Y [mm]	Z [mm]	3D [mm]	X [mm]	Y [mm]	Z [mm]	3D [mm]
		3.3	-0.2	-1.5	3.6	0.4	0.1	-0.0	0.4
i	Accuracy check on reference bars					X [mm]	Y [mm]	Z [mm]	3D [mm]
l	Area around point 6					0.3	0.3	0.5	0.7
m	Area around points 7 and 9					0.9	0.4	0.05	1.0
n	Area around point 8					0.9	0.5	0.1	1.1
o	<div> <p>● Camera position</p> <p>Images redundancy</p> <p>■ &gt; 9</p> <p>■ 9</p> <p>Discrepancy on GCPs</p> <p>● 5 mm</p> <p>● 4 mm</p> <p>● 3 mm</p> <p>● 2 mm</p> <p>● 1 mm</p> <p>● 0 mm</p> <p>● -1 mm</p> <p>● -2 mm</p> <p>● -3 mm</p> <p>● -4 mm</p> <p>● -5 mm</p> <p>Ellipse=error X and Y, color= error Z</p> </div> <div>  </div>								

(\*) high quality settings in dense point cloud reconstruction

(\*\*) medium quality settings in dense point cloud reconstruction

distributed throughout the test area and were mainly associated with the outer surfaces of coral colonies where the growth of corals is greatest. The color scale represents distances of 30 mm in yellow that are considered reasonable values of growth. Distances equal to and higher than 50 mm are shown in red and may be more related to the comparison of the 3D models than to higher values of coral growth. Negative difference values exceeding  $-50$  mm appear in blue (Fig. 4c). These negative values are more sparse than positive values and appear to be restricted to areas of little coral cover. The map also clearly points out small blue portions representing

the displacement of corals at the whole colonies level due to natural or anthropogenic events.

The multi-temporal comparison based on our distance calculation is well suited to detect main areal trends and provide measures of growth as well as areas of coral loss. More detailed analyses require the creation of vertical sections of the 3D models and the punctual comparison of the two profiles through a manual measurement of the point distances (Fig. 5). Figure 5a, b focuses on small portions of the mapped site: black lines specify the chosen vertical sections; white arrows indicate the viewing direction for the extracted profiles. Figure 5c shows

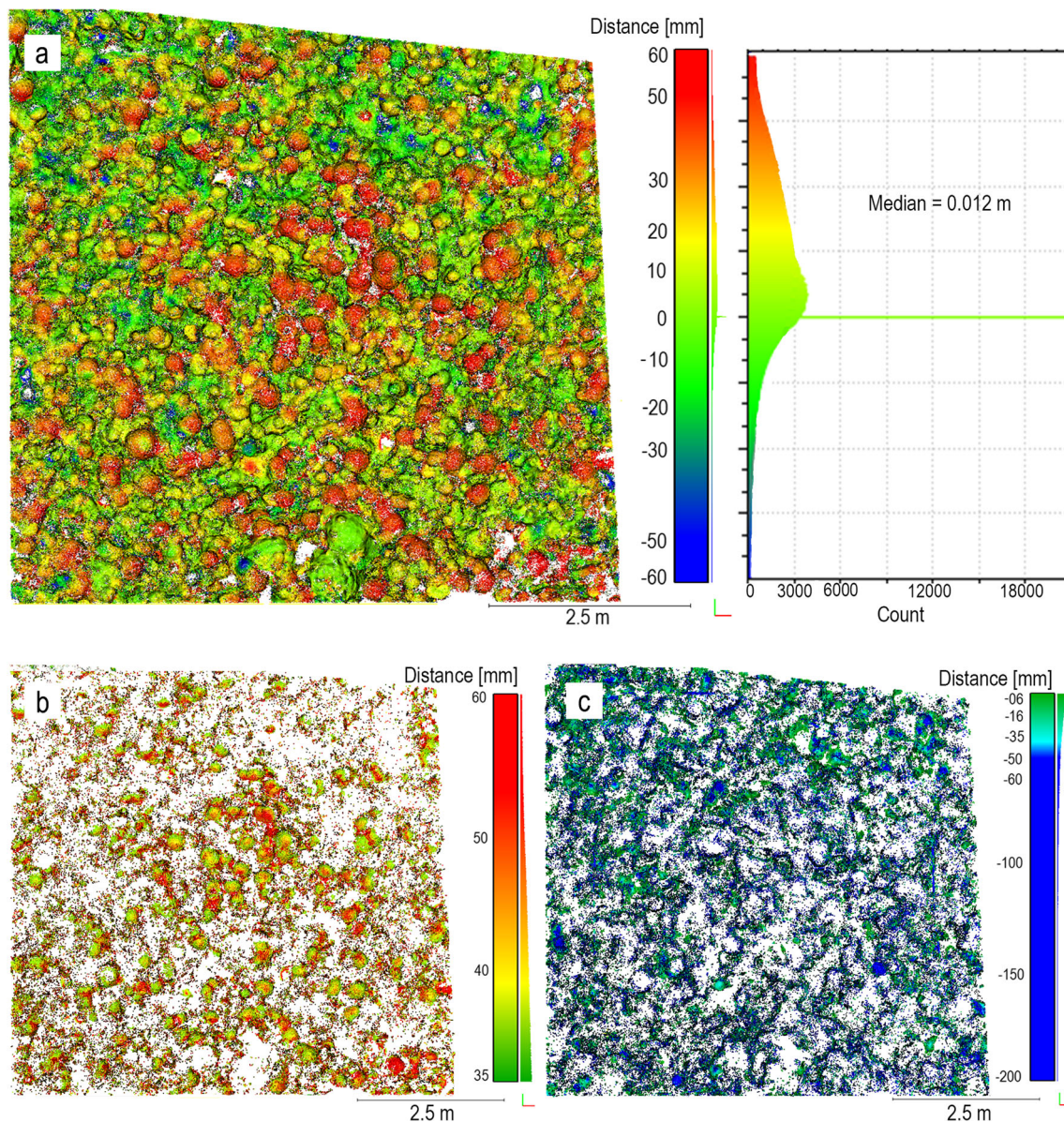


**Fig. 4** Comparison and coordinate variations between the 2017 model (reference) and the 2018 model (compared) as projected on the 2017 model. **a** Map of calculated distances (values between  $\pm 60$  mm), distribution of values and statistical parameters. **b** Extraction of large positive

values ( $> 35$  mm, 85th percentile), yellow color states 30 mm values. **c** Extraction of largest negative values (between  $-200$  and  $-6$  mm, the 15th percentile) to better report damaged coral concretions

a specific area of Section 2 that was selected in both models and displayed with natural colors in order to facilitate the comparison between the two models. Blue values represent negative distances, in this case corresponding to a loss of material related to the breakage of a coral colony; the detached material lays on the seabed close to the damaged area and is visible as a red area in the map (see area around Section 2 in Fig. 5a). The results obtained with the automatic distance calculation, as performed with M3C2 algorithm, were confirmed in terms of average changes. There is a good geometric agreement between the two models (see extracted profiles at the bottom of Fig. 5). Positive distances are bigger at the top of the coral colonies

and decrease on the sides. In red areas, manually identified distances are maximally 30–35 mm. Breakages of coral can lead to high negative distances (i.e.,  $-135$  mm shown in Section 2) as well as occlusions that, in vertical walls and narrow valleys, decrease the accuracy of the reconstruction.

## Discussion

As previously discussed, the role of the geodetic network is essential for the definition of an unequivocal reference frame that allows for the multi-temporal comparison and



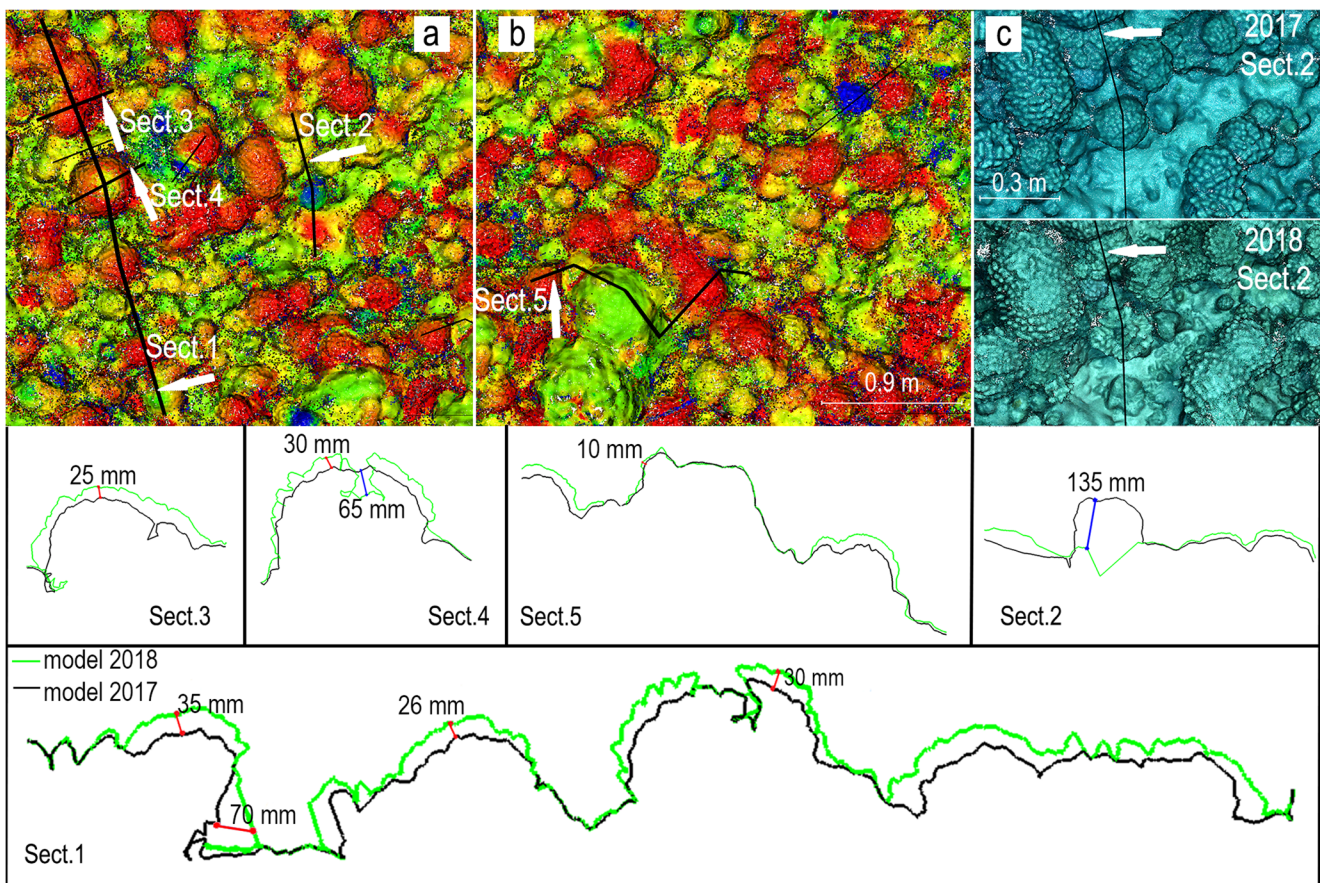


**Fig. 5** Multi-temporal comparison—detailed analyses: vertical sections of the two models. **a, b** Maps of the extracted sections in black lines and white arrows indicating the view direction. **c** View of the two models around Sect. 2. At the bottom, n. 5 extracted profiles with punctual measures of changes

the determination of the magnitude and the geometrical features of changes in the 3D structure of a coral reef. By the introduction of accurate GCP coordinates obtained from a least square adjustment, the 3D models produced by the photogrammetric process are directly and immediately comparable with no need to introduce other data manipulations (such as adaptation procedures) that would compromise the reliability of the final comparison between single epoch dataset. In this study, a full datum definition was achieved by the introduction of a point of constraint and an orientation. Specifically, we used average distances between GCPs to improve the accuracy of observations in the adjustment procedure. This limits the redundancy of adjusted observations and reduces the chances of overestimation of the final accuracy of our GCPs with more reliable results in successive multi-temporal comparison of surfaces representing the habitat evolution as changes in reef 3D geometry. Our strategy used in the datum definition (i.e., a bringing to minimally constrained reference system) relies on the need to adopt a common and stable reference system to frame solutions at successive epochs and, thus, preserve continuity in monitoring actions even in

case of a lost GCPs through time. This is an essential condition whenever 3D models are to be used in a monitoring program.

The presented datasets are based on different capturing strategies following improvements that had been adopted during our 2018 field mission. Specifically, the photoacquisition distance was reduced between 2017 and 2018, the camera was aligned with an off-nadir position and the diver operating the camera swam a regular grid pattern above the area of interest guaranteeing higher covering and redundancy. This reduced the mean ground resolution from 1.3 mm/pix in 2017 to 0.5 mm/pix in 2018, resulting in different features within the generated point clouds. Changes in the dense point cloud creation settings allowed us to obtain products with a similar number of points and resolution. The profiles shown in Fig. 5 highlight a similar capability of the two products in the reconstruction of small details. The lower number of images in the 2017 dataset also affected the robustness of the reconstruction geometry reducing the usable information and variability of viewing angles per reconstructed points (James et al. 2017). Not all reconstructed areas in the final

products are related to occlusions during images acquisition, areas of no data were located mainly in valleys between coral colonies (Fig. 4c) and affected the comparison of the two 3D models. Collecting images from a greater distance above the reef ensured an excellent coverage of the area but provided a lower ground resolution that may not produce the accuracy desired in the final reconstruction. Collecting images from a distance closer to the reef surface in a convergent way, ensures a higher resolution in the reconstruction, but some narrow valleys may not be fully detected because of the reduced frame area and the complex 3D geometry of the reef. The acquisition of images from different distances above the reef structures (for instance in a range from 2 to 5 m) could overcome these critical issues. We plan to test such a solution during our planned 2019 surveys. Increasing the distances of acquired images could improve the relative orientation of images, ensuring the coverage of a large area, whereas images closer to the objects will guarantee the high quality and resolution of generated 3D models.

Discrepancies in the GCPs coordinates (see Table 2, line h) represent the adjustment of the 3D model to imposed external constraints; values of 3.6 mm and 0.4 mm were found for the 2017 and 2018 datasets, respectively. These differences may be related to unstable reference points or differences in the image collection. If the reference points are unstable, coordinates measured in 2018 would not fit the 2017 dataset and this could lead to larger discrepancies in GCPs. The stability of the reference system forms the basic hypothesis of a geodetic reference network and is mandatory for reliable multi-temporal comparisons. Thus, the geodetic network needs to be periodically verified in order to avoid misinterpretation of the results of the final multi-temporal comparisons. Considering the short time between our two campaigns and the method by which the benchmarks were installed, it is reasonable to assume that the GCPs were not subject to changes or modifications and are therefore stable. In the long term, their continued stability should be confirmed by repeating the ground measurements in order to verify the consistency of their coordinates. In our case, the most probable cause of the observed variations in the positions of the GCPs (line h of Table 2) was the different protocols used to acquire the 2017 and 2018 imagery. The acquisition geometry affects the accuracy of the entire 3D reconstruction (Harwin et al. 2015). As suggested by James and Robson (2012) for aerial photogrammetric applications, the higher acquisition distance used in 2017 likely reduced the precision in CGP target identification and lessened the overall accuracy of the generated 3D model for that year.

The direct comparison of the two generated 3D point clouds indicates that the two reconstructions were well aligned. The algorithm for the automatic calculation of oriented distances

between point clouds highlights the main trends (Fig. 4a), with growth areas located near the tops of the coral colonies (Fig. 4b). It should be noted that the comparison of 3D point clouds between years does not constitute a deformation monitoring process in and of itself, as it is not possible to unambiguously identify the exact same point in space at two different times and follow its evolution. The M3C2 algorithm tries to solve these issues by defining thresholds for the measured values as well as search directions that are functions of the 3D surface geometry. This approach allows the investigation of the prevailing changes in reef 3D architecture; it is a very effective, automatic, and fast method to evaluate growth trends and the average behavior of different coral colonies. However, calculated distances are not suitable for a precise quantitative assessment of changes over time. For observations and quantitative evaluations of changes related to specific points in reef 3D architecture, it is necessary to create sections and compare the extracted 2D profiles. In this way, an expert operator is able to identify the homologous points of interest and make specific measurements between them. As discussed above, distances measured on profiles are more consistent and representative of the investigated phenomenon and do not exceed +35 mm even in areas where the M3C2 algorithm generically gives values in excess of 45 mm.

Analysis carried out on the results of the multi-temporal comparison allowed us to evaluate the uncertainty of the comparison and to detected distances that can be reasonably interpreted as coral growth or dissolution, thus avoiding misinterpretation of 3D model errors that do not correspond to actual changes in reef geometry. The multi-temporal results provided by the comparison of the 2D profiles are affected by the accuracies of each profile. Given the difficulties introduced by the underwater environment, it was not possible to establish a methodology to provide this accuracy check. The system based on the use of known reference bars was initiated in 2018 and allowed us to verify the accuracy of the 3D model through external independent reference devices for this year only. Our accuracy check provided a final magnitude of about 1 mm (a value greater than the GCPs discrepancy given by the photogrammetric process), so it is reasonable to consider the accuracy of 2018 3D model equal to few millimeters. Concerning the 2017 3D model, in the absence of any external reference bars and taking into account the GCP discrepancies, we feel that a final accuracy of 1 cm is a reasonable estimate. Based on the variance propagation law, the multi-temporal comparison is affected by an error of about  $\pm 1$  cm. The purpose of this analysis was to provide a general framework used to identify only those areas of the reef that actually experienced growth or dissolution greater than the error inherent in our 3D models. Our analysis allows us to confidently conclude that differences greater or lesser than 1 cm



between the 2017 and 2018 models may represent a change in the 3D architecture of the investigated coral reef. The accuracy check employing reference bars used in this case study represents an empirical process for the estimation of a 3D model accuracy, but the results provided have proven to be very effective and this method will be repeated during our next survey campaign.

## Conclusions

This paper represents one of the first examples of quantifying changes in the complex 3D structure of a coral reef over a scale of tens of meters. Such an ability is crucial to the monitoring of coral reef ecosystems in the face of anthropogenic perturbations and impacts related to climate change. The results discussed above were obtained due to a robust protocol utilizing accurate and precise instrumentation as well as the rigorous adherence to developed procedures. This included the use of a camera and lens system with a great enough resolution to detect expected changes in the 3D architecture of the reef and the fixing of the focal length of the lens during the survey to keep all internal calibration parameters of the camera constant.

An accurate and precisely described geodetic network played a primary role in our ability to compare two or more 3D representations of the reef. The choice of a proper camera, the homogeneous realizations of reference points in the investigated area and in stable locations together with following a rigorous set of protocols for image processing allowed us to generate an accurate 3D product with high resolution. The approach to change detection proposed in this paper through the comparison of subsequent 3D models allows the removal of common systematic errors (Ogundare 2015). The use of the same GCP coordinates, the minimal constraint reference network, similar “flight” paths, together with the repetition of subsequent surveys under similar environmental conditions (summer months), are all strategies allowing managers to remove errors related to instrumentations, observers, sea currents, refraction indices, and seasonal variations.

Our proposed, underwater photogrammetric methodology allows for a cost-effective approach to the quantitative assessment of coral growth or dissolution with an estimated accuracy and a resolution suitable for the monitoring of coral accretion or dissolution of about 10/15 mm/year. Our methodology is effective and requires relatively little effort in the field beyond the initial effort required to install reference points and collect the measurement needed to accurately estimate the geodetic network with the desired level of accuracy.

**Acknowledgments** We would like to thank R. J. Schmitt and S. J. Holbrook, UC Santa Barbara, as well as A. Gruen and M. Troyer, ETH Zurich, for their contributions to this project. We also would like to thank E. Nocerino and F. Neyer, ETH Zurich, for thoughtful discussions and advice on data processing. Research was completed under permits issued by the French Polynesian Government (Délégation à la Recherche) and the Haut-commissariat de la République en Polynésie Française (DTRT) (Protocole d’Accueil 2005–2018).

**Funding** This work was partially supported by the U.S. National Science Foundation under Grant No. OCE 16-37396 (and earlier awards) as well as a generous gift from the Gordon and Betty Moore Foundation

## References

- Adam TC, Brooks AJ, Holbrook SJ, Schmitt RJ, Washburn L, Bernardi G (2014) How will coral reef fish communities respond to climate-driven disturbances? Insight from landscape-scale perturbations. *Oecologia* 176:285–296
- Agüera-Vega F, Carvajal-Ramírez F, Martínez-Carricondo P (2016) Accuracy of digital surface models and orthophotos derived from unmanned aerial vehicle photogrammetry. *J Surv Eng* 04016025. [https://doi.org/10.1061/\(ASCE\)SU.1943-5428.0000206](https://doi.org/10.1061/(ASCE)SU.1943-5428.0000206)
- Bellwood DR, Hughes TP, Folke C, Nystrom M (2004) Confronting the coral reef crisis. *Nature* 429:827–833
- Bessat F, Buigues D (2001) Two centuries of variation in coral growth in a massive Porites colony from Moorea (French Polynesia): a response of ocean-atmosphere variability from south Central Pacific. *Palaeogeogr Palaeoclimatol Palaeoecol* 175(1):381–392
- Bryson M, Ferrari R, Figueira W, Pizarro O, Madin J, Williams S, Byrne M (2017) Characterization of measurement errors using structure-from-motion and photogrammetry to measure marine habitat structural complexity. *Ecol Evol* 7(15):5669–5681
- Burns JHR, Delparte D, Gates RD, Takabayashi M (2015) Integrating structure-from-motion photogrammetry with geospatial software as a novel technique for quantifying 3D ecological characteristics of coral reefs. *PeerJ* 3:e1077
- Capra A (1993) Non-conventional system in underwater photogrammetry. *Int Arch Photogramm Remote Sens* 29:234–234
- Capra A, Dubbini M, Bertacchini E, Castagnetti C, Mancini F (2015) 3D reconstruction of an underwater archaeological site: comparison between low cost cameras. *ISPRS-international archives of the photogrammetry. Remote Sens Spat Inf Sci* 40(5W5):67–72
- Capra A, Castagnetti C, Dubbini M, Gruen A, Guo T, Mancini F, Neyer F, Rossi P, Troyer M (2017) High accuracy underwater photogrammetric surveying. In 3rd IMEKO international conference on metrology for archaeology and cultural heritage-MetroArchaeo 2017:696–701
- Cinner JE, Maire E, Huchery C, MacNeil MA, Graham NAJ, Mora C, McClanahan TR, Barnes ML, Kittinger JN, Hicks CC, D’Agata S, Hoey A, Gurney GG, Feary DA, Williams I, Kulbicki M, Vigliola L, Wantiez L, Edgar GJ, Stuart-Smith RD, Sandin SA, Green A, Hardt MJ, Beger M, Friedlander A, Wilson SK, Brokovich E, Brooks AJ, Cruz-Motta JJ, Booth DJ, Chabanet P, Gough C, Tupper M, Ferse SCA, Sumaila UR, Pardede S, Mouillot D (2018) The gravity of human impacts mediates coral reef conservation gains. *Proc Natl Acad Sci* 115(27):E6116–E6125
- Collin A, Hench JL, Pastol Y, Planes S, Thiault L, Schmitt RJ, Holbrook SJ, Troyer M, Davies N (2018) Very high resolution mapping of coral reef state using airborne bathymetric LiDAR surface-intensity and drone imagery. *Int J Remote Sens* 2018:109–119
- Drap P, Merad D, Seinturier J, Mahiddine A, Peloso D, Boi J M, Garrabou J (2013) Underwater programmetry for archaeology and

- marine biology: 40 years of experience in Marseille, France. In 2013 Digital Heritage International Congress (DigitalHeritage) Vol. 1, pp 97–104)
- Edmunds PJ (2017) Unusually high coral recruitment during the 2016 El Nino in Mo'orea French Polynesia. *PLoS One* 12(10):e0185167
- Eltner A, Kaiser A, Castillo C, Rock G, Neugirg F, Abellán A (2016) Image-based surface reconstruction in geomorphometry – merits, limits and developments. *Earth Surf Dynam* 4(2):359–389. <https://doi.org/10.5194/esurf-4-359-2016>
- Fabricus KE, Noonan SHC, Abrego D, Harrington L, De'ath G (2017) Low recruitment due to altered settlement substrata as primary constraint for coral communities under ocean acidification. *Proc R Soc B Biol Sci* 284(1862):20171536
- Ferrari R, Bryson M, Bridge TJ, Williams SB, Byrne M, Figueira W (2016) Quantifying the response of structural complexity and community composition to environmental change in marine communities. *Glob Chang Biol* 22:1965–1975
- Ferrari R, Figueira WF, Pratchett MS, Boube T, Adam A, Kobelkowsky-Vidrio T, Doo S, Atwood TB, Byrne M (2017) 3D photogrammetry quantifies growth and external erosion of individual coral colonies and skeletons. *Sci Rep* 7:16737
- Figueira W, Ferrari R, Weatherby E, Porter A, Hawes S, Byrne M (2015) Accuracy and precision of habitat structural complexity metrics derived from underwater photogrammetry. *Remote Sens* 7(12):16883–16900
- Fonstad MA, Dietrich JT, Courville BC, Jensen JL, Carbonneau PE (2013) Topographic structure from motion: a new development in photogrammetric measurement. *Earth Surf Proc Land* 38(4):421–430. <https://doi.org/10.1002/esp.v38.4>
- Gardner TA, Cote IM, Gill JA, Grant A, Watkinson AR (2003) Long-term region-wide declines in Caribbean corals. *Science* 301:958–960
- Guo T, Capra A, Troyer M, Gruen A, Brooks A J, Hench J L, Schmitt R L, Holbrook S J, Dubbini M (2016) Accuracy assessment of underwater photogrammetric three dimensional modelling for coral reefs. *ISPRS-Int Arch Photogramm Remote Sens Spat Inf Sci* 41
- Harwin S, Lucier A, Osborn J (2015) The impact of the calibration method on the accuracy of point clouds derived using unmanned aerial vehicle multi-view stereopsis. *Remote Sens* 7(9):11933–11953. <https://doi.org/10.3390/rs70911933>
- Hattori A, Shibuno T (2015) Total volume of 3S small patch reefs reflected in aerial photographs can predict total species richness of coral reef damselfish assemblages on a shallow back reef. *Ecol Res* 30(4):675–682
- Holbrook SJ, Schmitt RJ, Adam TC, Brooks AJ (2016) Coral reef resilience, tipping points and the strength of herbivory. *Sci Rep* 6:35817
- Holbrook SJ, Adam TC, Edmunds PJ, Schmitt RJ, Carpenter RC, Brooks AJ, Lenihan HS, Briggs CJ (2018) Recruitment drives spatial variation in recovery rates of resilient coral reefs. *Sci Rep* 8:7338
- Hughes TP, Kerry JT, Álvarez-Noriega M, Álvarez-Romero JG, Anderson KD, Baird AH, Babcock RC, Beger M, Bellwood DR, Berkelmans R, Bridge TC, Butler IR, Byrne M, Cantin NE, Comeau S, Connolly SR, Cumming GS, Dalton SJ, Diaz-Pulido G, Eakin CM, Figueira WF, Gilmour JP, Harrison HB, Heron SF, Hoey AS, Hobbs J-P, Hoogenboom MO, Kennedy EV, Kuo C-Y, Lough JM, Lowe RJ, Liu G, McCulloch MT, Malcolm HA, McWilliam MJ, Pandolfi JM, Pears RJ, Pratchett MS, Schoepf V, Simpson T, Skirving WJ, Sommer B, Torda G, Wachenfeld DR, Willis BL, Wilson SK (2017) Global warming and recurrent mass bleaching of corals. *Nature* 543:373–377
- James M R, Robson S (2012) Straightforward reconstruction of 3D surfaces and topography with a camera: accuracy and geoscience application. *J Geophys Res Earth Surf* 117(F3)
- James MR, Robson S, Smith MW (2017) 3-D uncertainty-based topographic change detection with structure-from-motion photogrammetry: precision maps for ground control and directly georeferenced surveys. *Earth Surf Proc Land* 42(12):1769–1788
- Johnson-Roberson M, Pizarro O, Williams SB, Mahon I (2010) Generation an visualization of large-scale three-dimensional reconstructions from underwater robotic surveys. *J Field Robot* 27(1):21–51. <https://doi.org/10.1002/rob.20324>
- Kayal M, Lenihan HS, Brooks AJ, Holbrook SJ, Schmitt RJ, Kendall BE (2018) Predicting coral community dynamics using multi-species population dynamics models. *Ecol Lett* 21(12):1790–1799
- Kocak DM, Caimi FM (2005) The current art of underwater imaging with a glimpse of the past and vision of the future. *Mar Technol Soc J* 39(3):5–26. <https://doi.org/10.4031/002533205787442576>
- Lague D, Brodu N, Leroux J (2013) Accurate 3D comparison of complex topography with terrestrial laser scanner: application to the Rangitikei canyon (NZ). *ISPRS J Photogramm Remote Sens* 82: 10–26
- Lenihan HS, Hench JL, Holbrook SJ, Schmitt RJ, Potoski M (2015) Hydrodynamics influence coral performance through simultaneous direct and indirect effects. *Ecology* 96(6):1540–1549
- Mancini F, Dubbini M, Gattelli M, Stecchi F, Fabbri S, Gabbianelli G (2013) Using unmanned aerial vehicles (UAV) for high-resolution reconstruction of topography: the structure from motion approach on coastal environments. *Remote Sens* 5(12):6880–6898. <https://doi.org/10.3390/rs5126880>
- Menna F, Nocerino E, Fassi F, Remondino F (2016) Geometric and optic characterization of a hemispherical dome port for underwater photogrammetry. *Sensors* 16(1):48
- Mora C (2008) A clear human footprint in the coral reefs of the Caribbean. *Proc R Soc B-Biol Sci* 275:767–773
- Nex F, Remondino F (2014) UAV for 3D mapping applications: a review. *Appl Geomat* 6(1):1–15
- Neyer F, Nocerino E, Gruen A (2018) Monitoring coral growth- the dicotomy between underwater photogrammetry and geodetic control network. *ISPRS Int Arch Photogramm Remote Sens Spat Inf Sci* 42(2)
- Ogundare JO (2015) Precision surveying: the principles and geomatics practice. John Wiley & Sons, pp 267–328
- Palma M, Casado MR, Pantaleo U, Cerrano C (2017) High resolution orthomosaics of African coral reefs: a tool for wide-scale benthic monitoring. *Remote Sens* 9(7):705
- Pennisi E (2002) Survey confirms coral reefs are in peril. *Science* 297: 1622b–1623b
- Reichert J, Schellenberg J, Schubert P, Wilke T (2016) 3D scanning as a highly precise, reproducible, and minimally invasive method for surface area and volume measurements of scleractinian corals. *Limnol Oceanogr Methods* 14(8):518–526
- Rossi P, Mancini F, Dubbini M, Mazzone F, Capra A (2017) Combining nadir and oblique UAV imagery to reconstruct quarry topography: methodology and feasibility analysis. *Eur J Remote Sens* 50(1):211–221
- Royer JP, Nawaf MM, Merad D, Saccone M, Bianchimani O, Garrahou J, Drap P (2018) Photogrammetric surveys and geometric processes to analyse and monitor red coral colonies. *J Mar Sci Eng* 6(2):42
- Rupnik E, Nex F, Remondino F (2014) Oblique multi-camera systems– orientation and dense matching issues. *ISPRS Int Arch Photogramm Remote Sens Spat Inf Sci* 40(3):107. <https://doi.org/10.5194/isprsarchives-XL-3-W1-107-2014>
- Sarakinoui I, Papadimitriou K, Georgoula O, Patias P (2016) Underwater 3D modeling: image enhancement and point cloud filtering. *ISPRS Int Arch Photogramm Remote Sens Spat Inf Sci* 41
- Skarlatos D, Agrafiotis P, Menna F, Nocerino E, Remondino F (2017) Ground control networks for underwater photogrammetry in archaeological excavations. In Proceedings of the 3rd IMEKO International Conference on Metrology for Archaeology and Cultural Heritage. MetroArcheo 2017 October 23–25, 2017, Lecce, Italy
- Snavely N, Seitz SM, Szeliski R (2006) Photo tourism: exploring photo collections in 3D. *ACM T Graph* 25(3):835–846

- Suchley A, Alavarez-Filip L (2018) Local human activities limit marine protection efficacy on Caribbean coral reefs. *Conserv Lett* 11(5): UNSPe12571
- Toschi I, Rivola R, Bertacchini E, Castagnetti C, Dubbini M, Capra A (2013) Validation tests of open-source procedures for digital camera calibration and 3D image-based modelling. *ISPRS Int Arch Photogramm Remote Sens Spat Inf Sci XL-5/W2*:647–652. <https://doi.org/10.5194/isprsarchives-XL-5-W2-647-2013>
- Trapon ML, Pratchett MS, Adjeroud M, Hoey AS, Baird AH (2013) Post-settlement growth and mortality rates of juvenile scleractinian corals in Moorea, French Polynesia versus Trunk Reef, Australia. *Mar Ecol Prog Ser* 488:157–170

**Publisher's note** Springer Nature remains neutral with regard to jurisdictional claims in published maps and institutional affiliations.